

## Structural properties depicted by optical measurements in hydrogenated polymorphous silicon

This article has been downloaded from IOPscience. Please scroll down to see the full text article.

1999 J. Phys.: Condens. Matter 11 8749

(<http://iopscience.iop.org/0953-8984/11/44/313>)

View [the table of contents for this issue](#), or go to the [journal homepage](#) for more

Download details:

IP Address: 171.66.16.220

The article was downloaded on 15/05/2010 at 17:46

Please note that [terms and conditions apply](#).

## Structural properties depicted by optical measurements in hydrogenated polymorphous silicon

S Vignoli<sup>†§</sup>, R Butté<sup>†</sup>, R Meaudre<sup>†</sup>, M Meaudre<sup>†</sup> and P Roca i Cabarrocas<sup>‡</sup>

<sup>†</sup> Département de Physique des Matériaux (UMR 5586 CNRS), Université Lyon I,  
43 Boulevard du 11 novembre 1918, 69622 Villeurbanne Cédex, France

<sup>‡</sup> Laboratoire de Physique des Interfaces et des Couches Minces (UMR 7647 CNRS),  
École Polytechnique, 91128 Palaiseau Cédex, France

E-mail: svignoli@dpm.univ-lyon1.fr

Received 21 July 1999

**Abstract.** Hydrogenated polymorphous silicon (pm-Si:H) is a new material obtained by plasma-enhanced chemical vapour deposition by running the plasma close to powder formation. Preliminary studies have revealed the presence of silicon nanocrystallites embedded in an amorphous matrix but only in a limited range of deposition conditions. In this work we have investigated the structural properties of such films by means of spectroscopic optical measurements. The analysis of transmission spectra in the transparent region has shown that pm-Si:H films have indeed a more ordered structure than state-of-the-art hydrogenated amorphous silicon (a-Si:H) films. This has been observed in the whole range of deposition conditions leading to pm-Si:H films. On a final point the implication of structural properties on the excellent optoelectronic properties previously reported in pm-Si:H films is discussed.

### 1. Introduction

It is well known that by plasma-enhanced chemical vapour deposition (PECVD) one can deposit hydrogenated amorphous silicon (a-Si:H) as well as hydrogenated microcrystalline silicon ( $\mu$ c-Si:H) by varying deposition conditions. In an intermediate regime, close to powder formation, a heterogeneous material is obtained now called hydrogenated polymorphous silicon (pm-Si:H) [1]. These pm-Si:H films are deposited using high hydrogen dilution of silane, high pressure and RF power. pm-Si:H films are heterogeneous in the sense that they contain nanometre size Si crystallites embedded in an amorphous matrix [1]. This peculiar structure has been evidenced by direct observations using high-resolution transmission electron microscopy (HRTEM) and Raman spectroscopy [2] but only in a limited range of deposition conditions leading to pm-Si:H films. Moreover pm-Si:H has been shown to be a very promising material for photovoltaic devices [3] since it presents very good optoelectronic properties and stability versus light induced degradation [4]. Therefore it is essential to obtain structural information in order to understand the enhanced optoelectronic properties of pm-Si:H.

To shed some light on the structure of pm-Si:H films in the whole range of deposition pressures we performed optical measurements by means of Fourier transform infrared (FTIR) spectroscopy, visible and near infrared (VIS–NIR) transmission spectroscopy and spectroscopic ellipsometry in the ultraviolet–visible (UV–VIS) range. It is well known that

§ Corresponding author.

optical measurements are powerful tools to depict weak structural or compositional variations in thin films. In particular the analysis of transmission spectra in the VIS–NIR range allows the determination of an average gap representative of the degree of compositional and/or topological disorder. In this paper we shall show that pm-Si:H films have indeed a more ordered network compared to standard a-Si:H and that their structural properties are intermediate between those of  $\mu$ c-Si:H and a-Si:H.

## 2. Samples and experimental details

Samples were prepared in a PECVD reactor by RF (13.56 MHz) glow discharge [5]. a-Si:H films with up-to-grade electronic properties were prepared by decomposition of pure silane at a substrate temperature of 250 °C on Corning 7059 glass substrate with a power density of 5 mW cm<sup>-2</sup> and at a total pressure of 5 Pa leading to a deposition rate  $r_d \approx 1 \text{ \AA s}^{-1}$ . A strongly hydrogen diluted silane, i.e. SiH<sub>4</sub> diluted to 2% in H<sub>2</sub>, is used as the reactant gas source to deposit pm-Si:H films at a substrate temperature of 150 °C with a power density of 90 mW cm<sup>-2</sup>. The total pressure was varied in a wide range from 148 to 293 Pa and the resulting deposition rate is of the order of 1 Å s<sup>-1</sup>.

VIS–NIR transmission measurements were carried out with a Perkin Elmer  $\lambda$  900 double beam spectrophotometer on samples deposited on Corning 7059 glass substrates in the 500–2500 nm range. Hydrogen contents were determined from FTIR spectroscopy by using a Perkin Elmer spectrum 2000 spectrophotometer by integrating the absorption band at 640 cm<sup>-1</sup> [6] of samples deposited on c-Si substrates in order to reduce the interference fringes. We have checked by elastic recoil detection analysis (ERDA) that the same proportionality factor applies to both pm-Si:H and a-Si:H films when determining the hydrogen content from the absorption band at 640 cm<sup>-1</sup>. Finally spectroscopic ellipsometry measurements were carried out on samples deposited either on Corning 7059 glass or c-Si substrates with a Sopra ES4G rotating analyser ellipsometer in the 1.5–4.95 eV range. We underline the fact that for a given sample the deposition on various substrates was realized in the same run.

In table 1 we have reported some deposition parameters as well as some physical parameters deduced from our measurements (see below).

**Table 1.** Deposition conditions and relevant parameters.  $d$  is the thickness of our samples deduced either from mechanical or optical measurements.  $E_{04}$  is the energy at which the absorption coefficient reaches the value of 10<sup>4</sup> cm<sup>-1</sup> as deduced from VIS–NIR transmission spectra.  $E_p$  and  $n_0$  are the Penn gap and the static refractive index respectively determined by the dispersion behaviour of the refractive index in the sub-gap region (see the text).  $C_H$  is the content of bonded hydrogen deduced from FTIR spectra.

Samples	$T_s$ (°C)	% SiH <sub>4</sub>	Pressure		$d$ ( $\mu$ m)	$E_p$ (eV)	$E_{04}$ (eV)	$n_0$	$C_H$ (%)
			(Pa)						
810081	150	2	160		0.72	3.620	2.05	3.371	20.3
810082	150	2	202		0.73	3.594	2.02	3.418	20.3
810083	150	2	239		0.86	3.614	1.98	3.427	19.0
810092	150	2	266		0.89	3.625	1.98	3.404	19.5
810093	150	2	293		0.63	3.546	1.97	3.444	19.2
901251	150	2	207		0.78	3.627	1.94	3.378	19.2
901261	150	2	173		1.53	3.645	1.96	3.391	15.7
901262	150	2	200		1.88	3.598	2.00	3.382	15.0
901271	150	2	148		1.09	3.668	2.01	3.324	15.4
912201	100	100	5		0.70	3.482	1.89	3.320	15.0
902023	250	100	5		1.40	3.486	1.89	3.476	8.0

### 3. Results and discussion

Figure 1 displays a typical transmission spectrum in the VIS–NIR range for a pm-Si:H sample. A careful analysis of the interference fringes enables the determination of the dispersion of the refractive index  $n$  in the sub-gap region as well as the thickness of the samples [7, 8]. For this latter quantity a very good agreement was found between the values determined by optical and mechanical (stylus profilometry) measurements. In figure 2 we have plotted  $n(h\nu)$  obtained from the above analysis and from spectroscopic ellipsometry data versus photon energy. The latter shows interference fringes in the low energy range arising from the mismatch of the refractive indexes between the substrate (c-Si in this case) and the film. Both sets of data are in very good agreement and the interference fringes present in the ellipsometry spectrum are well averaged by the data deduced from VIS–NIR transmission measurements. However spectroscopic ellipsometry measurements integrate the dielectric function of the material under study and the effects of surface roughness (particularly at high photon energies) and of the substrate (at low energy, when the absorption coefficient of the material is low, the film cannot be considered as semi-infinite). Therefore only the pseudo-optical constants are obtained [9]. The ellipsometry data presented in figure 2 have been corrected for the substrate influence but not for the surface roughness. The reason for this is that a precise knowledge of the dielectric response of Si nanocrystallites embedded in an absorbing medium is necessary in order to correctly model our films. The surface roughness is usually modelled by a mixture of the bulk material and voids so no attempts have been made at the time of writing. But we emphasize that samples studied do not present a ‘milky’ surface, which is a signature of rough surface [10]. Moreover we have checked by means of atomic force microscopy (AFM) that surface roughness is similar in both pm-Si:H and a-Si:H films, thus making a direct comparison possible between these two kinds of film. In addition the shape of the spectrum in figure 1 clearly indicates that surface roughness is very weak and if this were not the case the interference pattern would be rapidly destroyed [8].

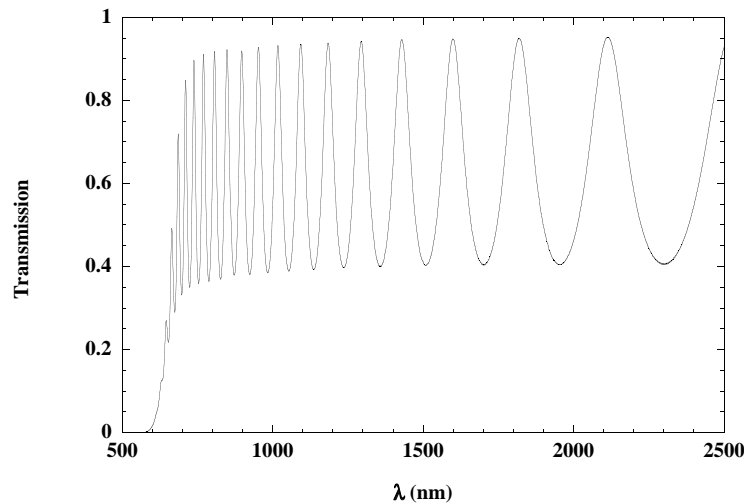
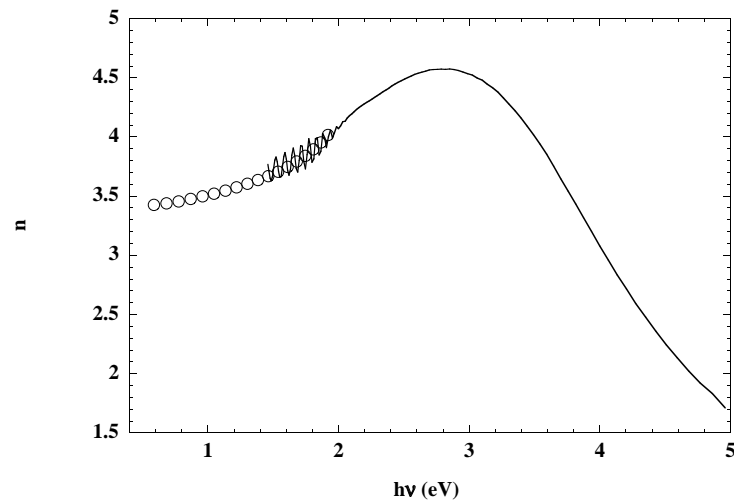


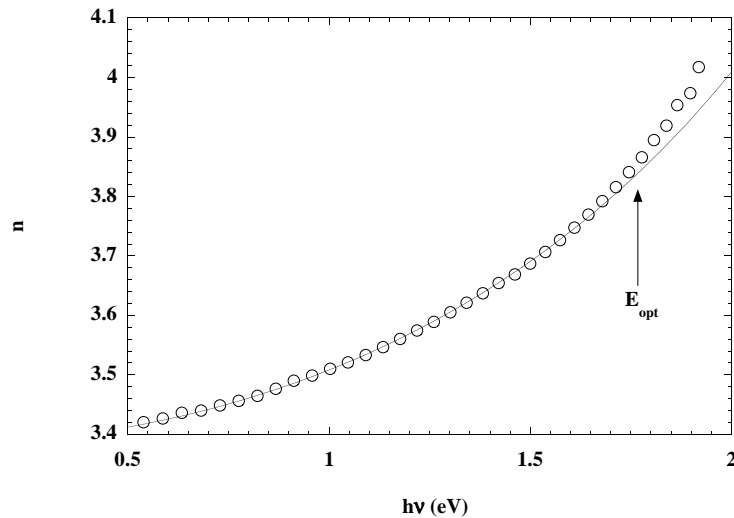
Figure 1. VIS–NIR transmission spectrum for a pm-Si:H film (901262).

In the single oscillator approach and assuming a delta function for the imaginary part of the dielectric function  $\varepsilon_2$  at energy  $E_p$ , we have in the sub-gap region

$$n^2(h\nu) - 1 = \frac{E_0^2}{E_p^2 - (h\nu)^2} \quad (1)$$

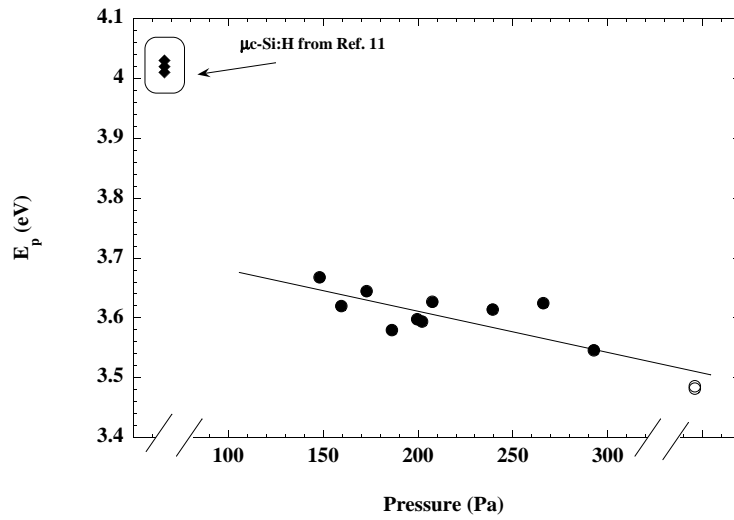


**Figure 2.** Refractive index  $n$  deduced from VIS-NIR transmission ( $\circ$ ) and from spectroscopic ellipsometry (solid line) for sample 901262.



**Figure 3.** Refractive index  $n$  for sample 901262. The line is a fit to equation (1). Note this fit has been performed only in the sub-gap region although the data obtained on the whole range are presented. The arrow indicates the value of the optical gap deduced from a Tauc plot of the absorption coefficient.

where  $h\nu$  is the photon energy,  $E_0$  the plasma energy and  $E_p$  an average gap often referenced as the Penn gap [11]. This last quantity gives a measure of the energy difference of the ‘centres of gravity’ of the valence and conduction bands and therefore gives information on the overall band structure. In figure 3 we have plotted the refractive index versus the photon energy for a pm-Si:H film. A very good fit is obtained from equation (1) and a clear departure from the one-oscillator approximation is observed when the film becomes absorbing as expected. All the films studied here present the same behaviour as one shown in figure 3.



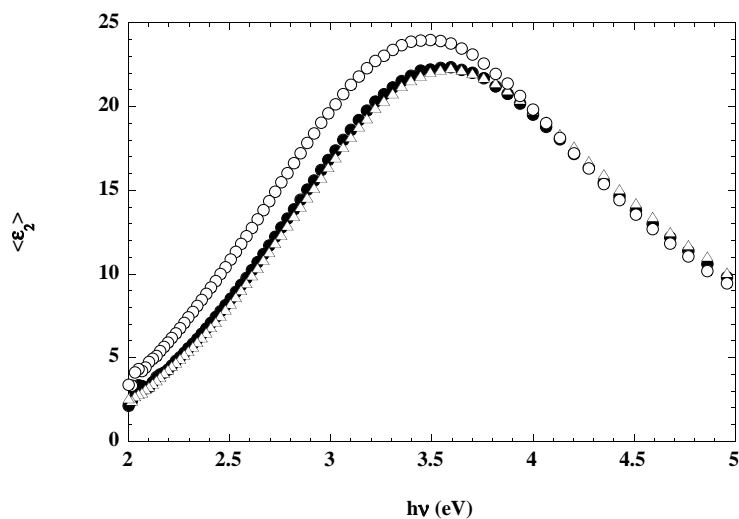
**Figure 4.** Penn gap  $E_p$  versus the deposition pressure for pm-Si:H films (●). Data for  $\mu\text{c-Si:H}$  (◆) samples and two a-Si:H (○) films deposited at 250 and 100 °C have been added for comparison. The line is a guide to the eye.

Figure 4 is a plot of  $E_p$  versus the deposition pressure of pm-Si:H films. For comparison we have added values of  $E_p$  for a standard device-grade a-Si:H deposited at 250 °C and for  $\mu\text{c-Si:H}$  obtained by Remeš *et al* [11] with crystalline fraction of the order of 80%. One clearly observes a continuous decrease of  $E_p$  when going from pm-Si:H to a-Si:H. This behaviour is well supported by the decrease of the energy of the maximum in  $\langle \varepsilon_2 \rangle$  spectra,  $\langle \varepsilon_{2\text{max}} \rangle$ , shown in figure 5, and by the decrease of  $E_{04}$ , the energy at which the absorption coefficient  $\alpha$  reaches the value of  $10^4 \text{ cm}^{-1}$  (see table 1). Moreover a linear relation between  $E_p$  and  $E_{04}$  is expected in tetrahedrally bonded semiconductors [12]

$$E_p \approx E_{04} + \Delta \quad (2)$$

where  $\Delta$  is a constant equal to 1.5–2 eV. The Penn gap is plotted as a function of  $E_{04}$  in figure 6 and it denotes that a scaling up of the overall band structure arises in our pm-Si:H films. However equation (2) is only approximately verified in our samples. We emphasize that these two quantities probe very different states. Thus  $E_{04}$  is very sensitive to the states near the band edges whereas  $E_p$  determined from equation (1) is rather unaffected by these states. The use of a more sophisticated model to fit  $n(h\nu)$  taking account the finite bandwidth of the conduction and valence bands will improve the determination of  $E_p$ . Such an analysis has been performed on a-SiC:H films by Solomon [13] to remove the quantitative discrepancy between photoemission and VIS–NIR transmission results [14] although qualitatively the behaviour is the same when using equation (1). However the use of equation (4) of the paper of Solomon [13] would lead to a four parameter fit and comparison to recently published data [11] would be no longer possible.

In amorphous semiconductors the Penn gap was shown to depend on various structural parameters such as coordination number, bond length and bond angle distortion although the latter is believed to have only minor effects [15] as well as on film composition in a-SiC:H films [14] and in  $\mu\text{c-Si:H}$  and a-Si:H [11]. Therefore one could argue that the high hydrogen content in our pm-Si:H films (see table 1) is responsible for the increase in  $E_p$  values due to an alloying effect. To elucidate this point we have determined the Penn gap for an a-Si:H film



**Figure 5.** Imaginary part of the pseudo-dielectric function for a-Si:H sample deposited at 250 °C (○) and two pm-Si:H samples 901262 (△) and 810092 (●). Only two pm-Si:H films are represented for clarity but we emphasize that all pm-Si:H samples behave similarly.

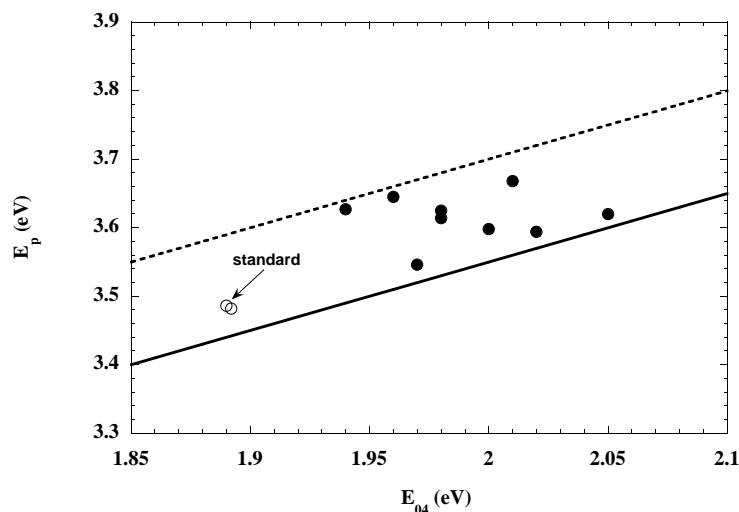


**Figure 6.** Penn gap  $E_p$  versus the energy  $E_{04}$  at which the absorption reaches the value of  $10^4 \text{ cm}^{-1}$ . The lines correspond to equation (2) with  $\Delta$  values of 1.55 eV (solid line) and 1.7 eV (dashed line).

deposited at 100 °C in the same conditions as described before. At this deposition temperature the hydrogen content is at least 15% [16] that is approximately the same content as in our pm-Si:H films. The Penn gap for this low quality a-Si:H film is notably lower than in pm-Si:H. In addition Remeš *et al* [11] have shown by a similar analysis that  $E_p$  was indeed higher in their  $\mu\text{c-Si:H}$  samples even if they contain less hydrogen than in their glow discharge a-Si:H films. Thus we attribute the increase of the Penn gap in our pm-Si:H films to a more ordered structure compared to conventional a-Si:H in the whole range of deposition pressures. Although Si nanocrystallites were directly observed by means of high resolution transmission electron microscopy (HRTEM) and Raman spectroscopy for pm-Si:H samples elaborated at

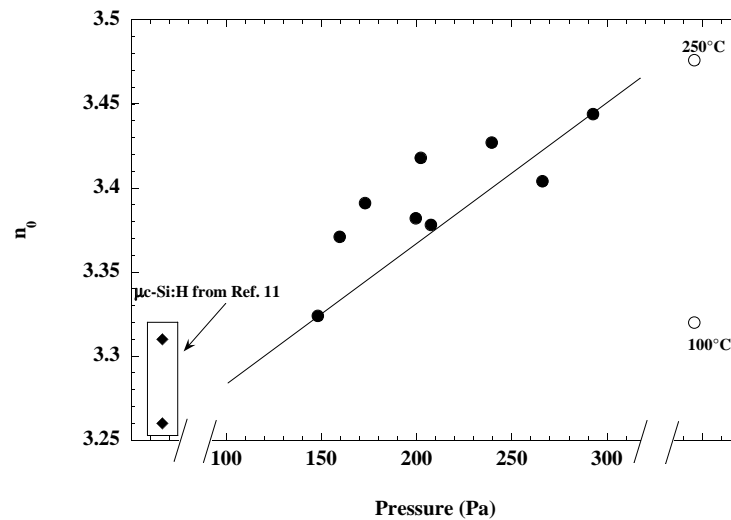


**Figure 7.** Static refractive index versus the deposition pressure for pm-Si:H films (●). Data for  $\mu\text{c-Si:H}$  (◆) samples and two a-Si:H (○) films deposited at 250 and 100 °C have been added for comparison. The line is a guide to the eye.

the lower deposition pressure [2], direct structural investigations fail to show the presence of nanocrystallites or at least ordered regions for higher deposition pressures due probably to their smaller proportion or sizes.

We turn now the discussion on the behaviour of the static refractive index  $n_0$  as function of the deposition pressure for our pm-Si:H films. The results are displayed in figure 7 where data for  $\mu\text{c-Si:H}$  [11] and for our a-Si:H films have been added. It is usually found in a-Si:H that a high hydrogen content decreases  $n_0$  and the density of the corresponding film [11, 17]. These observations are accompanied by a decrease of  $\langle \varepsilon_{2\text{max}} \rangle$  although this quantity indicates only qualitative variations of density [18]. This density decrease is commonly explained by the appearance of microvoids and polyhydride configurations when increasing the hydrogen content as revealed by an infrared stretching absorption band centred at around  $2100\text{ cm}^{-1}$ .

Therefore one could naïvely think that our pm-Si:H films have a lower density than up-to-grade a-Si:H films (see figures 5 and 7 and table 1). However the situation is not so clear. Indeed the stretching band in FTIR spectra measured in our films cannot be decomposed into two bands centred at  $2000$  and  $2100\text{ cm}^{-1}$  as it is usually the case in a-Si:H films with a high hydrogen content. We effectively find two stretching absorption bands but centred at  $2000$  and  $2030\text{ cm}^{-1}$  [1–3]. The latter has been ascribed to a peculiar hydrogen bonding configuration, namely hydrogen platelets [19], suggesting a rather different hydrogen incorporation in pm-Si:H films. The absence of an absorption band at  $2100\text{ cm}^{-1}$  or in other words the absence of microvoids or polyhydride configurations has been confirmed by preliminary small angle x-ray scattering (SAXS) performed in our group. Moreover Tsu *et al* [20] have calculated the static dielectric constant  $\varepsilon_0$  in Si clusters by using a modified Penn model. Their results clearly indicate a decrease in  $\varepsilon_0$  when decreasing the cluster size, e.g. a reduction of 22% and 4% in  $\varepsilon_0$  values as compared to the bulk value are found for cluster sizes of 20 and  $50\text{ \AA}$  respectively which is the range of Si crystallites observed in pm-Si:H films deposited at low pressures [2]. Thus in the framework of the effective medium approximation a decrease in  $n_0$  would be expected in pm-Si:H material and this decrease would be more pronounced when increasing the crystalline



fraction as shown in figure 7. Moreover the study of Remeš *et al* [11] on  $\mu\text{c-Si:H}$  and  $\text{a-Si:H}$  shows that there is no unique behaviour of  $n_0$  with the density. Thus the high hydrogen content and the behaviour of  $n_0$  will not necessarily indicate a decrease in density for  $\text{pm-Si:H}$  films due to the peculiar hydrogen incorporation and to the presence of Si crystallites. Thus direct measurements of the density are required before concluding on this point.

Finally we would like to discuss the implication of the more ordered network in  $\text{pm-Si:H}$  films on their optoelectronic properties. By plotting the normalized photoconductivity  $\eta\mu\tau$  of  $\text{pm-Si:H}$  films versus the deposition pressure a 'bell shape'-like curve is obtained [2, 4]. That means when going from low pressures ( $\sim 150$  Pa) to higher ones ( $\sim 300$  Pa) the  $\eta\mu\tau$  product first increases to reach a maximum for pressure in the range 200–250 Pa and then decreases. This behaviour has been observed for both the annealed state and after light-induced degradation. This has been explained by a preferential carrier recombination path on dangling bonds located at Si nanocrystallites surfaces for which the capture cross section is expected to be lower than in  $\text{a-Si:H}$  films due to the confinement [2]. Moreover this decrease in the dangling bond capture cross sections for  $\text{pm-Si:H}$  films has recently been observed by means of space charge relaxation measurements [21]. Thus based on the results of figure 4 we expect smaller crystallites and even the disappearance of the latter leading to an improved amorphous matrix when increasing the deposition pressure. Since the capture cross sections decrease when decreasing the crystallites size [22] we can expect an increase in  $\eta\mu\tau$  first and then a decrease when increasing the deposition pressure leading to an optimized deposition pressure in terms of photoconductivity and stability versus light-induced degradation. This is precisely what we observed in our preliminary studies.

#### 4. Conclusion

In conclusion we have shown that it is possible to obtain substantial information on the structure of hydrogenated polymorphous silicon by optical measurements in the sub-gap region. The use of very simple experimental techniques and analysis makes this procedure very attractive when direct structural observations are difficult. The main result is that hydrogenated polymorphous silicon exhibits a better ordered structure compared to up-to-grade hydrogenated amorphous silicon despite its high hydrogen content. These observations confirm previously reported results obtained by means of HRTEM and Raman spectroscopy but only for a limited range of deposition conditions. However more works are needed to elucidate the precise link between the excellent optoelectronic properties of this new material and its structure.

#### Acknowledgments

We gratefully acknowledge J P Chapel from the Laboratoire des Matériaux Polymères et des Biomateriaux (UMR 5627 CNRS) for his help during spectroscopic ellipsometry and AFM measurements. This work was supported by Centre National de la Recherche Scientifique and Agence pour le Développement et la Maîtrise de l'Énergie (ECODEV program).

#### References

- [1] Roca i Cabarrocas P 1998 *Amorphous and Microcrystalline Silicon Technology (Mater. Res. Soc. Symp. Proc. 507)* ed R Schropp *et al* (Pittsburgh, PA: Materials Research Society) p 855
- [2] Butté R, Saviot L, Marty O, Vignoli S, Meaudre R, Meaudre M and Roca i Cabarrocas P 1999 *Phys. Rev. B* at press

- [3] Roca i Cabarrocas P, Hamma S, St'ahel P, Longeaud C, Kleider J P, Meaudre R and Meaudre M 1997 *Proc. 14th Eur. Photovoltaic Solar Energy Conf. Exhibition (Barcelona)* ed H A Ossenbrink, P Helm and H Ehmann (Bedford: Stephens) p 1444
- [4] Butté R, Meaudre R, Meaudre M, Vignoli S, Longeaud C, Kleider J P and Roca i Cabarrocas P 1999 *Phil. Mag. B* **79** 1079
- [5] Roca i Cabarrocas P, Chevrier J B, Huc J, Lloret A, Parey J Y and Schmitt J P M 1991 *J. Vac. Sci. Technol. A* **9** 2331
- [6] Langford A A, Fleet M L, Nelson B P, Lanford W A and Maley N 1992 *Phys. Rev. B* **45** 13 367
- [7] Swanepoel R 1983 *J. Phys. E: Sci. Instrum.* **16** 1214
- [8] Swanepoel R 1984 *J. Phys. E: Sci. Instrum.* **17** 896
- [9] Dréysson B 1993 *Prog. Cryst. Growth Characterization Mater.* **27** 1
- [10] Vaněček M, Poruba A, Remeš Z, Beck N and Nesládek M 1998 *J. Non-Cryst. Solids* **227–230** 967
- [11] Remeš Z, Vaněček M, Torres P, Kroll U, Mahan A H and Crandall R S 1998 *J. Non-Cryst. Solids* **227–230** 876
- [12] Weaire D and Thorpe M F 1971 *Phys. Rev. B* **4** 2508
- [13] Solomon I 1997 *Phil. Mag. B* **76** 273
- [14] Solomon I, Schmidt M P, Sénémaud C and Driss Khodja M 1988 *Phys. Rev. B* **38** 13 263
- [15] Paul W, Connell G A N and Temkin R J 1973 *Adv. Phys.* **22** 531
- [16] Roca i Cabarrocas P, Djebbour Z, Kleider J P, Longeaud C, Mencaraglia D, Sib J, Bouizem Y, Thèye M L, Sardin G and Stoquert J P 1992 *J. Physique* **2** 1979
- [17] Remeš Z, Vaněček M, Mahan A H and Crandall R S 1997 *Phys. Rev. B* **56** R12 710
- [18] Haage T, Schmidt U I, Fath H, Hess P, Schröder B and Oechsner H 1994 *J. Appl. Phys.* **76** 4894
- [19] von Keudell A and Abelson J R 1998 *J. Appl. Phys.* **84** 489
- [20] Tsu R, Babić D and Ioriatti L 1997 *J. Appl. Phys.* **82** 1327
- [21] Meaudre R, Meaudre M, Butté R, Vignoli S 1999 *Phil. Mag. Lett.* **79** 767
- [22] Delerue C, Allan G and Lannoo M 1993 *Phys. Rev. B* **48** 11 024